Evolution of molar shape in didelphid marsupials (Marsupialia: Didelphidae): analysis of the influence of ecological factors and phylogenetic legacy

MARIA AMELIA CHEMISQUY[1,4]*, FRANCISCO J. PREVOSTI[1,2,4], GABRIEL MARTIN[3,4] and DAVID A. FLORES[1,4]

[1]*División Mastozoología, Museo Argentino de Ciencias Naturales 'Bernardino Rivadavia', Ciudad Autónoma de Buenos Aires, Argentina*
[2]*Departamento de Ciencias Básicas, Universidad Nacional de Luján, Luján, Buenos Aires, Argentina*
[3]*Laboratorio de Investigaciones en Evolución y Biodiversidad, Facultad de Ciencias Naturales Sede Esquel, Universidad Nacional de la Patagonia 'San Juan Bosco', Esquel, Chubut, Argentina*
[4]*Consejo Nacional de Investigaciones Científicas y Técnicas (CONICET), Ciudad Autónoma de Buenos Aires, Argentina*

The diversity of items consumed by modern didelphids, varying from mostly fruits in *Caluromys* Allen to mostly small vertebrates in *Lutreolina* O. Thomas, may cause changes in molar size and shape. We evaluated the morphometric variation of the first and third upper and lower molars of 16 genera of didelphid marsupials, with the aim of assessing the relationship between molar shape change, diet and phylogeny. We used a geometric morphometric approach to analyse how shape changes with diet. We mapped shape onto the phylogeny of the group to reconstruct ancestral states and analyse the evolution of molar shape. Finally, we statistically estimated the effect of size, diet and phylogeny on molar shape. All the analyses indicated little correlation between diet and molar shape and a strong correlation between the position of each genus on the phylogeny and molar shape. We believe that the wide ecological niche used by most of the groups (at least regarding diet) makes the evolutionary changes not strong enough to override pre-existing differences that occur among clades, and the absence of highly diet-specialized species (e.g. hypercarnivory or obligate folivory) causes the need for retaining a molar shape that can be useful to process different kinds of food items.

INTRODUCTION

Molars are complex structures that possess great variation among species, from simple conical structures in dolphins to complex molars with folds and transverse plates in capybaras (Ungar, 2010). As well as the other teeth, they play an important role in taxonomic analyses, and have been widely used to infer the diet of extinct species (e.g. Goin & Montalvo, 1988; Goin, Velázquez & Scaglia, 1992; Dumont, Strait & Friscia, 2000; Abello, Ortiz Jaureguizar & Candela, 2012), and also as characters for phylogenetic analyses (e.g. Reig, Kirsch & Marshall, 1987; Goin & Pardiñas, 1996; O'Leary & Geisler, 1999; Voss & Jansa, 2009; Prevosti, 2010; Archibald & Averianov, 2012; O'Leary *et al*., 2013). The basic tribosphenic molar is composed of an upper element with three pointed principal cusps (paracone, metacone and protocone) connected with cutting crests, and a lower element comprising the trigonid, or shearing end (also with three principal cusps and crests), and the talonid, or crushing heel (Luo, Cifelli &

*Corresponding author. E-mail: amelych80@gmail.com

Kielan–Jaworowska, 2001). In occlusal view, tribosphenic molars constitute a system able to perform different functions during mastication (Crompton & Hiiemae, 1969, 1970). The upper row forms a continuous series of triangles with their apices directed toward the middle line of the oral cavity. The triangular spaces formed by these structures are coupled by a series of inverted triangles formed by the trigonid of the inferior elements. In this way, the talonids of the inferior row contact the lingual (or inner) half of the superior elements (i.e. the protocone) (Crompton & Hiiemae, 1969, 1970).

The relative position of molar cusps and crests is the main characteristic to analyse when trying to infer diets, and many authors have developed different approaches that relate molar shape to diet. For example, Goin *et al*. (1992) analysed the orientation of the metacrista and the paracristid using the angle that those crests form with the mesiodistal axis of the molar series in Didelphoidea to differentiate between carnivores, insectivores and omnivores. Kay (1975) used the length of the shearing blades of the second lower molar to separate fruit-eating primates from leaf-eating primates. The same approach was followed by Strait (1993) to discriminate between insectivores feeding on hard and soft objects. New and more complex analyses use three-dimensional molar modelling to relate crest orientation and cusp size and shape with diet, taking into account the effects of occlusion and wear in molars (Evans, 2005; Evans & Sanson, 2006; Evans *et al*., 2007). All these contributions (and many others not mentioned for the sake of brevity) show that mammal molars can be good indicators of differences in diet habits, something that can be explained by their function in food processing.

Despite this relationship between molar shape and diet, there is a general agreement that the phylogenetic history of a group also influences molar morphology (e.g. Kay & Hylander, 1978; Strait, 1993; Caumul & Polly, 2005; Ungar, 2010; Klukkert, Teaford & Ungar, 2012). This explains why tooth morphology has been used for more than a century to classify and identify mammals, and to establish their phylogenetic relationships.

Didelphid marsupials have primitive tribosphenic molars, the upper ones with a well-developed buccal stylar shelf, and five stylar cusps (Meléndez, 1990; Hillson, 2005). Lower molars have a well-developed trigonid and talonid, and twinned entoconid and hypoconulid, which are well separated from the hypoconid (Meléndez, 1990; Ungar, 2010). The 'didelphoid' molar model is an ancient morphology already established in the Cretaceous (Fox, 1987). However, living didelphids and some Neogene extinct marsupials exhibit a relatively derived molar morphology with respect to most Cretaceous and Paleogene metatherians, such as a 'V-shaped' centrocrista (Reig *et al*., 1987; but see Case, Goin & Woodburne, 2005). Although within modern didelphids there are no major changes in molar morphology (Voss & Jansa, 2009), the diversity of items consumed by their members, from mostly frugivorous in *Caluromys* Allen to highly carnivorous in *Lestodelphys* Tate (Vieira & Astúa de Moraes, 2003), could be reflected in changes in molar size and shape, such as the relative position of crests and cusps (see, for example, Goin *et al*., 1992).

In this study, we evaluated the morphometric variation of the first and third upper and lower molars of 13 extant and three extinct genera of didelphid marsupials, with the main aim being to assess the relationship between molar shape change, diet and phylogeny. We used a traditional geometric morphometric approach to analyse how shape changes with diet. We also mapped shape onto the phylogeny of the group to reconstruct ancestral states and analyse the evolution of molar shape in Didelphidae. Finally, using an approach similar to canonical phylogenetic ordination (Giannini, 2003), we statistically estimated the effect of size, diet and phylogeny on the shape of the molars.

MATERIAL AND METHODS

SAMPLING

We digitized the first and third upper and lower molars of 103 specimens corresponding to 13 extant genera of Didelphidae and three extinct taxa, analysing as many representatives of each genus as we could (Table 1, see Supporting Information, Table S1). For the highly speciose genera *Marmosa* Gray, *Monodelphis* Burnett, *Philander* Brisson and *Thylamys* Gray we included representatives of more than one species. This was done to account for as much variation as possible within each genus, although molar morphology has been found mostly to be uniform for each (Voss & Jansa, 2009). Therefore, samples were pooled to show one general pattern per genus.

Goin *et al*. (1992) showed that there are no differences in tooth morphology between males and females in *Monodelphis dimidiata* (J.A. Wagner), one of the most dimorphic species within New World marsupials (Pine, Dalby & Matson, 1985). Moreover, Martin (2005) mentions the lack of sexual dimorphism for teeth in *Lestodelphys halli* (O. Thomas), derived from a very large dataset of upper and lower molars, while the same pattern is described for the genus *Thylamys* by Martin (2008). Therefore, we assumed that there is no sexual dimorphism in didelphid molars and included both sexes. Goin *et al*. (1992) also showed bilateral asymmetry between left and right molars. Consequently, we only digitized right molars. As teeth acquire full adult size from the start (Hillson, 2005), both juveniles and adults were included, selecting only molars with little wear.

Table 1. The number of specimens of each molar included per genus, and diet classification assigned to each genus (following Vieira & Astúa de Moraes, 2003)

Genus	M1	M3	m1	m3	Diet
Caluromys J.A.Allen	3	2	4	4	I
Chironectes Illiger	4	2	3	3	V
Cryptonanus Voss, Lunde & Jansa	4	2	6	4	II
Didelphis Linnaeus	11	9	11	7	III
Gracilinanus Gardner & Creighton	2	2	2	1	II
Hyperdidelphys Ameghino	2	2	2	1	V
Lestodelphys Tate	3	2	3	3	V
Lutreolina O. Thomas	9	4	7	6	V
Marmosa Gray	4	3	3	4	II
Marmosops Matschie	2	2	2	2	II
Metachirus Burmeister	4	3	4	4	IV
Monodelphis Burnett	10	6	8	9	IV
Philander Brisson	5	5	4	4	IV
Thylamys Gray	7	5	6	5	IV
Thylatheridium Reig	3	*	3	8	V
Thylophorops Reig	5	2	2	10	V

*This taxon was not included in the analyses of third upper molars due to excessive wear of the available materials.

Diet categories used for all analyses (Table 1) were based on Vieira & Astúa de Moraes (2003), who classified the genera of Neotropical marsupials in five ordered categories from mostly frugivorous (I) to mainly carnivorous species (V). Extinct genera were placed under the category V, as they are all described as highly carnivorous (Reig *et al.*, 1987; Goin & Montalvo, 1988; Goin & Pardiñas, 1996). Diet classification of fossil taxa is based mostly on dental anatomy, although sometimes considering different aspects of dentition from those analysed here (e.g. Goin *et al.*, 1992). Consequently, we might possibly fall in a circular argument when we include the diet information of extinct taxa in some of the analyses, inflating the relationship between diet and dental morphology. However, because we found that that was a weak relationship (see Results), we think that including extinct taxa is not necessarily problematic for our work and allows us to widen the taxonomic sample and the scope of our study.

IMAGES AND LANDMARKS

Molars in occlusal view were digitally imaged using a stereomicroscope with image capture capability. For both upper and lower molars, teeth were orientated placing the molar neck parallel to the lens plane. Images were carefully checked to avoid errors due to misorientation, and when necessary they were repeated until the right orientation was achieved. All images contained a scale.

Dental terminology (Fig. 1B, D) partially follows Voss & Jansa (2009). For upper molars, 26 landmarks and semi-landmarks were digitized on the following positions: 1, stylar cusp E (StE); 2–14, semi-landmarks describing the labial margin of the tooth; 15, apex of stylar cusp A (StA); 16, apex of stylar cusp B (StB); 17, apex of stylar cusp D (StD); 18, apex of the metacone; 19–24, semi-landmarks describing the centrocrista; 25, apex of the paracone; 26, apex of the protocone (Fig. 1A). For lower molars, 13 landmarks and semi-landmarks were digitized on the following positions: 1, apex of the hypoconid; 2, apex of the hypoconulid; 3, apex of the entoconid; 4, apex of the metaconid; 5, apex of the paraconid; 6, anterior border of the anterior cingulum; 7–11, semi-landmarks describing the anterobasal cingulum; 12, posterior border of the anterobasal cingulum; 13, apex of the protoconid (Fig. 1C). The application MakeFan6 (Sheets, 2003) was used to ensure consistent placement of the semi-landmark coordinates using an equiangular and equidistant criterion to place them, depending on the structure. In the case of upper molars, a 20-line fan was placed in the labial margin radiating from the most concave point of the centrocrista, and a 12-line comb was placed on the centrocrista from the paracone to the metacone. For lower molars, a 10-line fan was placed on the anterior cingulum radiating from the notch between paraconid and protoconid. Both landmarks and semi-landmarks were then digitized using the software tpsDIG 2.12 (Rohlf, 2008a). Unaligned landmark coordinates are available as Supporting information, Data S1.

MULTIVARIATE ANALYSES OF SHAPE

Landmark configurations were aligned by performing a Procrustes superimposition, using the program TPSrelw 1.46 (Rohlf, 2008b). For the alignment, semi-landmarks were slid using the minimum bending energy method (Bookstein, 1997). The distribution of specimens on shape space was analysed by performing a principal component analysis (PCA) of the Procrustes coordinates using the software MorphoJ (Klingenberg, 2011).

The relationship between tooth morphology and diet was explored using a between-group PCA, which projects the data onto the principal components of the group means (Mitteroecker & Bookstein, 2011). Between-group PCA leads to a better group separation than the ordinary PCA, but avoids the overfitting achieved by the canonical variate analysis and the linear discriminant analysis, and preserves the original Procrustes distances in the shape space produced by the superimposition (Mitteroecker & Bookstein, 2011; Seetah, Cardini & Miracle, 2012). Between-group PCA was performed using the package ade4 (Dray & Dufour, 2007) for the software R (R Development Core Team, 2012).
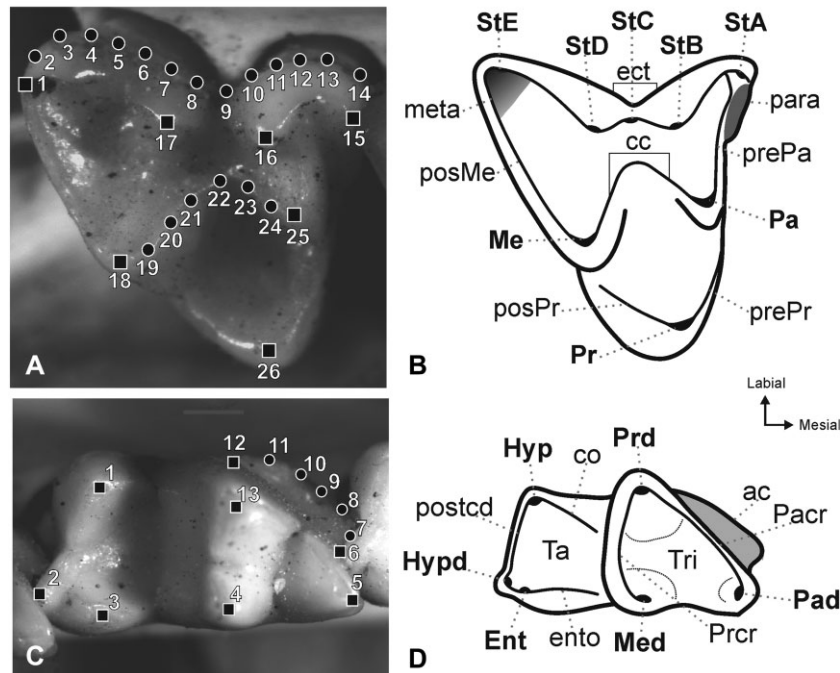
Figure 1. Occlusal views of the third upper (A, B) and lower (C, D) didelphid molars. A and C, molars of *Didelphis albiventris* showing the landmarks and semilandmarks used. B and D, didelphid molars illustrating features of crown morphology discussed in the text. Squares, landmarks; circles, semilandmarks. See text for a detailed description of landmarks. Abbreviations: ac, anterior cingulum (light grey shading); cc, centrocrista; co, cristid obliqua; ect, ectoflexus; Ent, entoconid; ento, entocristid; Hyp, hypoconid; Hypd, hypoconulid; Me, metacone; Med, metaconid; meta, metastylar corner (grey shading); Pa, paracone; Pacr, paracristid; Pad, paraconid; para, parastylar corner (dark grey shading); postcd, postcristid; prePa, preparacrista; Pr, protocone; Prcr, protocristid; Prd, protoconid; prePr, preprotocrista; posMe, metacrista; posPr, postprotocrista; StA, stylar cusp A; StB, stylar cusp B; StC, stylar cusp C; StD, stylar cusp D; StE, stylar cusp E; Ta: talonid; Tri: trigonid.

To analyse the shape transformation associated with the distribution in the between-group PCA, shape was regressed against the coordinates of each specimen on the first and second principal components (PC1 and PC2).

PHYLOGENETIC RECONSTRUCTION OF ANCESTRAL SHAPE

Landmark configurations were optimized on the phylogeny, through spatial optimization using maximum parsimony, as described by Catalano, Giannini & Goloboff (2010) and Goloboff & Catalano (2011). The algorithm optimizes the landmark configurations on phylogenetic trees using a modification of the Sankoff optimization (see Goloboff & Catalano, 2011). This method allows the reconstruction of the displacement of each landmark – in two dimensions in this case – as if they were independent 'characters'. The summation of individual landmark optimizations (i.e. the reconstruction of their ancestral position in each node) gives the ancestral landmark configuration of every node of the tree (for more details see Catalano

et al., 2010). We used the tree resulting from the analysis of five concatenated genes published by Voss & Jansa (2009: fig. 33). Extinct taxa (indicated by †) were placed following the final cladogram published by Reig *et al.* (1987: fig. 68) for *Thylatheridium*† Reig and *Thylophorops*† Reig, and the cladogram obtained by Goin & Pardiñas (1996) for *Hyperdidelphys*† Ameghino.

The optimization was performed using the software TNT (Goloboff, Farris & Nixon, 2008), using a grid of ten cells, a window of two cells and a nesting level of the grids of four. Although specimens were pre-aligned using a Procrustes superimposition, we also improved the alignments using a dynamic superimposition approach, which simultaneously superimposes and maps landmark configurations (Catalano & Goloboff, 2012).

CORRELATION BETWEEN SHAPE, SIZE, DIET AND PHYLOGENY

To evaluate the effect of phylogeny, size and diet on the shape, we used a method inspired by the canonical phylogenetic ordination proposed by Giannini (2003),

as it is the only comparative method that allows the partitioning of how much of the shape (a multidimensional variable) is explained by the factors mentioned above. The method consists of performing a redundancy analysis (RDA; Legendre & Legendre, 1998) using shape (i.e. the landmark configurations of the aligned specimens) as the community matrix and centroid size, diet and phylogeny as constraints. Phylogenetic information was taken from the matrix representation using parsimony of the tree (MRP), which consists of a binary matrix where the columns represent the membership of each taxon to a clade (see Giannini, 2003). We analysed the effect of the three factors together as constraints, of each factor separately as a constraint and the effect of each factor separately using the remaining factors as a conditioning matrix. This last analysis allowed us to evaluate the individual effect of each factor, excluding the interaction with the other variables (Legendre & Legendre, 1998). To discard collinear variables from the model we proceeded as follows: first, we evaluated the percentage of shape variation explained by each variable independently using an RDA (i.e. size, diet and each node of the phylogeny); second, we entered in the model the variable that explained the most variation and estimated the Akaike information criterion (AIC; Godínez-Domínguez & Freire, 2003) value for that model. Then, we entered in the model each of the remaining variables in order of explanation percentage until the AIC became constant. The variables that did not reduce the AIC were excluded from the final model.

To account for individual variation on the entire sample, but to avoid the effect of over-representing certain genera (as they had more specimens analysed), each of the RDAs was performed 10 000 times using a resampled matrix that included only one specimen randomly chosen per genus each time. Resampling of the data, RDAs with their significance and AIC estimations were performed using the R package vegan (Oksanen *et al*., 2013).

RESULTS

SHAPE ANALYSES

PC1 and PC2 of the analysis of the first lower molar (m1) explained 23.65 and 18.28% of the total variance, respectively. Specimens placed on the negative end of PC1 showed molars with a larger trigonid and a smaller talonid, a distal displacement of the protoconid and the metaconid, and a narrower anterior cingulum (Fig. 2), while the opposite trend was observed on the positive end of PC1. PC2 showed specimens with shorter molars on its negative end, with relatively longer trigonids and shorter talonids, and a more robust anterior cingulum (Fig. 2). On its positive end,

PC2 showed specimens with longer m1s and the opposite trend in the remaining characters (Fig. 2). The graph showed a broad superposition of taxa. However, it is important to note the placement of *Caluromys* on the upper left quadrant, *Lestodelphys* (with other specimens of Thylamyini) on the lower left quadrant, and *Metachirus* Burmeister and *Hyperdidelphys*† on the positive end of PC1 (Fig. 2). The other taxa were placed in intermediate positions of the graph, although in general terms, the Didelphini–Metachirini group tended to be separated on PC1 from the Thylamyini and Marmosini. No clear pattern of distribution was found between specimens and the different diet categories, except for category I, which was placed on the upper left quadrant by itself and separated from the others (Fig. S1).

PC1 and PC2 from the analysis of the first upper molar (M1) explained 28.41 and 16.54% of the total variance, respectively. Specimens placed on the negative end of PC1 showed molars with a shorter and transversally oriented metacrista, mesially displaced StD that is closer to StB, and a less pronounced ectoflexus (Fig. 3), while specimens placed on the positive end of the PC1 showed the opposite trend. The negative end of PC2 showed specimens with more symmetrical molars, with a shorter metacrista and paracrista, a more convex labial margin, a less inflected centrocrista and a distally displaced protocone (Fig. 3), while the opposite trend was observed on the positive end of PC2. In contrast to what was observed in the first lower molar, the PCA of the M1 showed less superposition of taxa. *Caluromys* was placed in the negative end of PC1, clearly separated from the remaining taxa. *Marmosa*, *Marmosops* Matschie and *Cryptonanus* Voss, Lunde & Jansa were placed on the positive end of PC2, while *Chironectes* Illiger was at the opposite end of the plot (Fig. 3). *Lestodephys*, *Hyperdidelphys*† and *Thylatheridium*† were placed on the lower right quadrant of the plot. The remaining taxa were placed in intermediate positions between these extremes (Fig. 3). Diet categories showed a broad superposition except for category I, placed on the negative end of PC1. There is almost no overlap between categories II and III, which are placed on the positive and negative ends of PC2, respectively. However, both categories are broadly overlapped by categories IV and V (Fig. S2).

In the analysis of the third lower molar (m3), PC1 and PC2 explained 34 and 16.83% of the total variance, respectively. The shape change observed along each axis was very similar to the change observed along PC1 and PC2 for m1 (Fig. 4). However, in this analysis, the distribution of the taxa changed compared with the analysis of m1, with *Lutreolina* Thomas, *Hyperdidelphys*†, *Thylatheridium*† and species of Thylamyini placed mostly on the negative side of PC1,
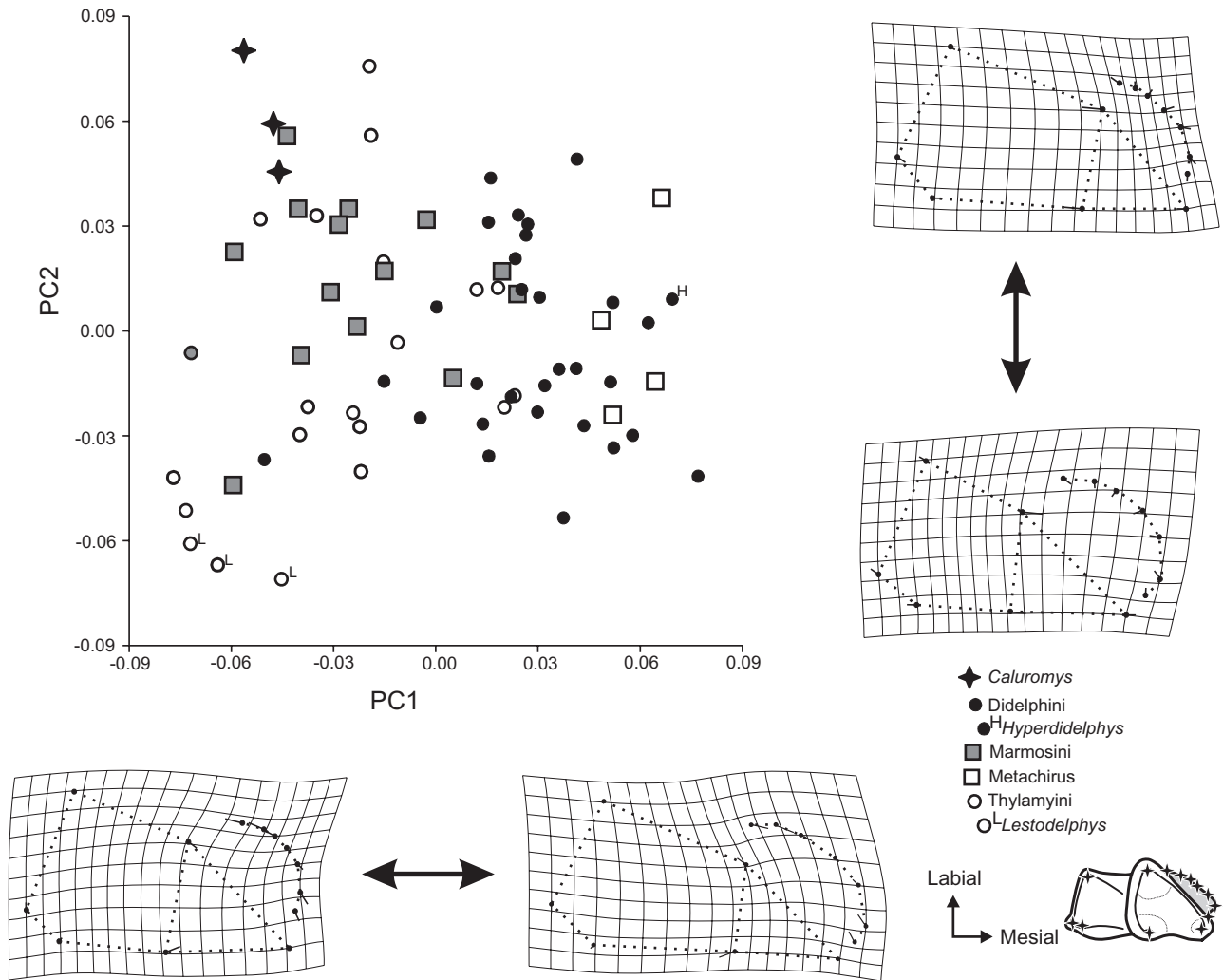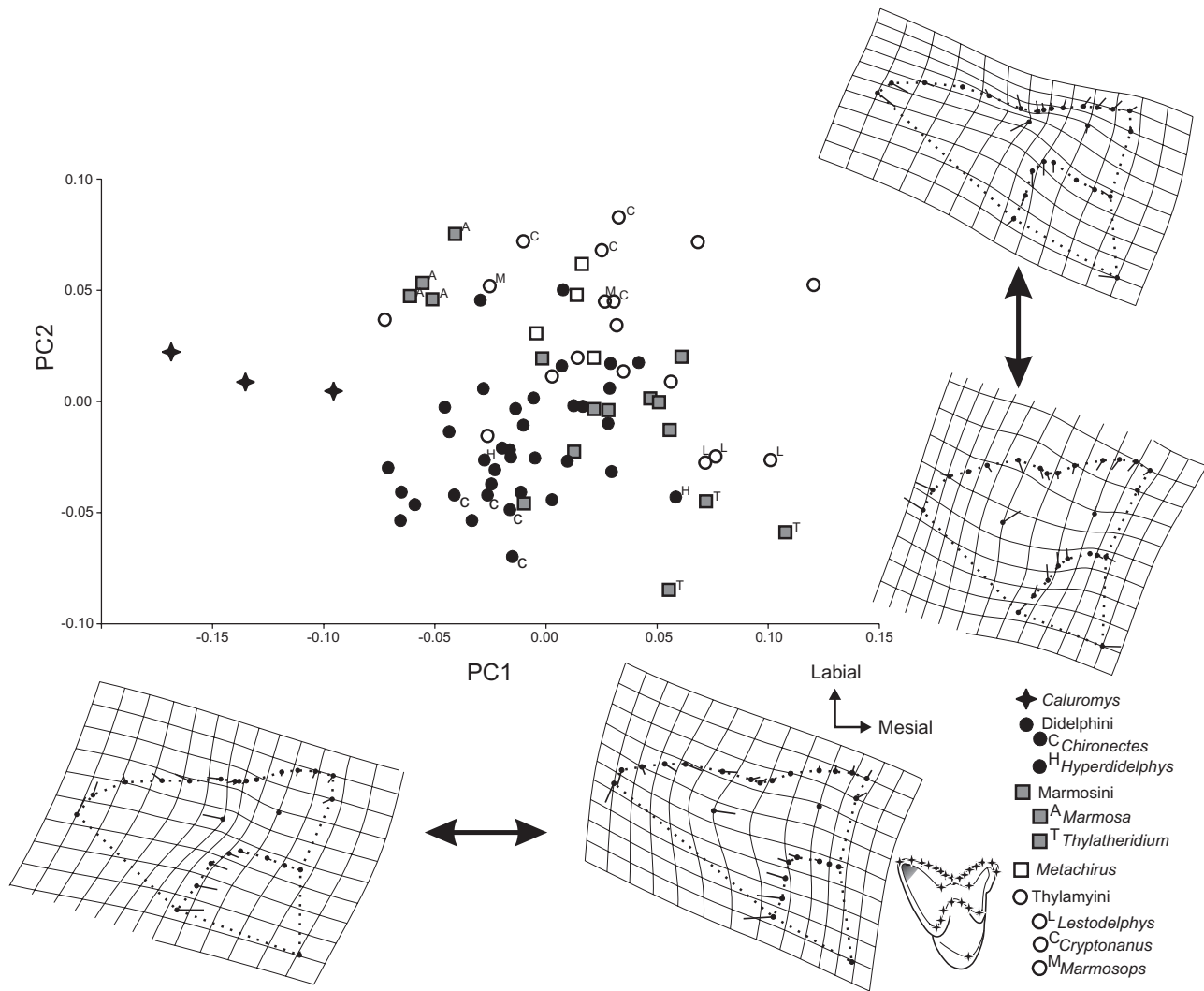
Figure 2. First lower molar (m1) shape variation along the first two principal components (PC) from the PCA of the Procrustes coordinates, showing the distribution of taxonomic groups. Deformation grids show the extreme shape of each PC.

other species of Didelphini on the positive end of PC1, *Caluromys* placed on the positive end of PC2 and *Metachirus* on the negative end (Fig. 4). Regarding diet categories, there was no clear ordination pattern, except for the placement of taxa within category I on the upper left quadrant. Note, however, a trend for taxa within category II to be placed on the negative end of PC1, and taxa of category III on the positive end of PC1. Nonetheless, there was a broad superposition among the five categories (Fig. S3).

In the analysis of the third upper molar (M3), PC1 and PC2 explained 35.47 and 21.29% of the total variance, respectively. Specimens placed on the negative end of PC1 showed a shorter M3, with a longer metacrista and paracrista, a labially displaced StB and StD, an expanded stylar shelf caused mainly by the lingual displacement of the paracone and the metacone,

a deeper ectoflexus and a more inflected centrocrista (Fig. 5). Specimens placed on the positive end of PC1 showed longer M3s, with the opposite pattern on the remaining characters (Fig. 5). On the negative end of PC2 specimens showed a distally displaced StA, mesially displaced StD, distolabially displaced StE, distolingually displaced metacone and a less inflected centrocrista, while specimens placed on the positive end of PC2 showed the opposite trend. *Didelphis* Linnaeus was placed on the positive end of PC1, near *Caluromys*, which was also placed on the positive end of PC2. Specimens of *Lutreolina*, *Hyperdidelphys*† and *Thylophorops*† were found on the negative end of PC2, while *Lestodelphys* was placed on the negative end of PC1 (Fig. 5). The remaining taxa were placed in intermediate positions throughout the different axes, with a trend towards the negative end of PC1 (Fig. 5). Regarding

Figure 3. First upper molar (M1) shape variation along the first two principal components (PC) from the PCA of the Procrustes coordinates, showing the distribution of taxonomic groups. Deformation grids show the extreme shape of each PC.

diet, categories I and III are separated from the remaining categories, on the positive end of PC2 and PC1, respectively. The remaining categories form a continuum, displaced to the negative end of PC1, from the negative end of PC2 for category V to the positive end of PC2 for categories II and IV (Fig. S4).

The effect of size on the PCAs was evaluated by regressing, for each data set, PC1 and PC2 with size (i.e. log centroid size). Except for PC2 of the m3 analysis, there was a significant correlation between shape and size in all the cases. However, the percentage of shape explained by size was low in most cases, and reached only 50% for PC1 of M3 (m1 42.97 and 12.87%; m3 19.82 and 1.13%; M1 7.96 and 25.59%; M3 53.12 and 23.64% for PC1 and PC2, respectively). Consequently, although allometry is playing a role in the distri-

bution of specimens on the plots, its effect is not strong and is not concentrated in only one of the principal components but is distributed in, at least, PC1 and PC2.

RELATIONSHIP BETWEEN TOOTH MORPHOLOGY AND DIET

On the between-group PCA (B-G PCA) of m1 we did not find an improvement of the results obtained by the PCA, showing a broad overlap among diet categories, with the exception of category I. This category was located on the negative end of PC1, apart from the remaining categories, with a morphological pattern that showed a smaller anterior cingulum and a broader trigonid (Fig. S5).
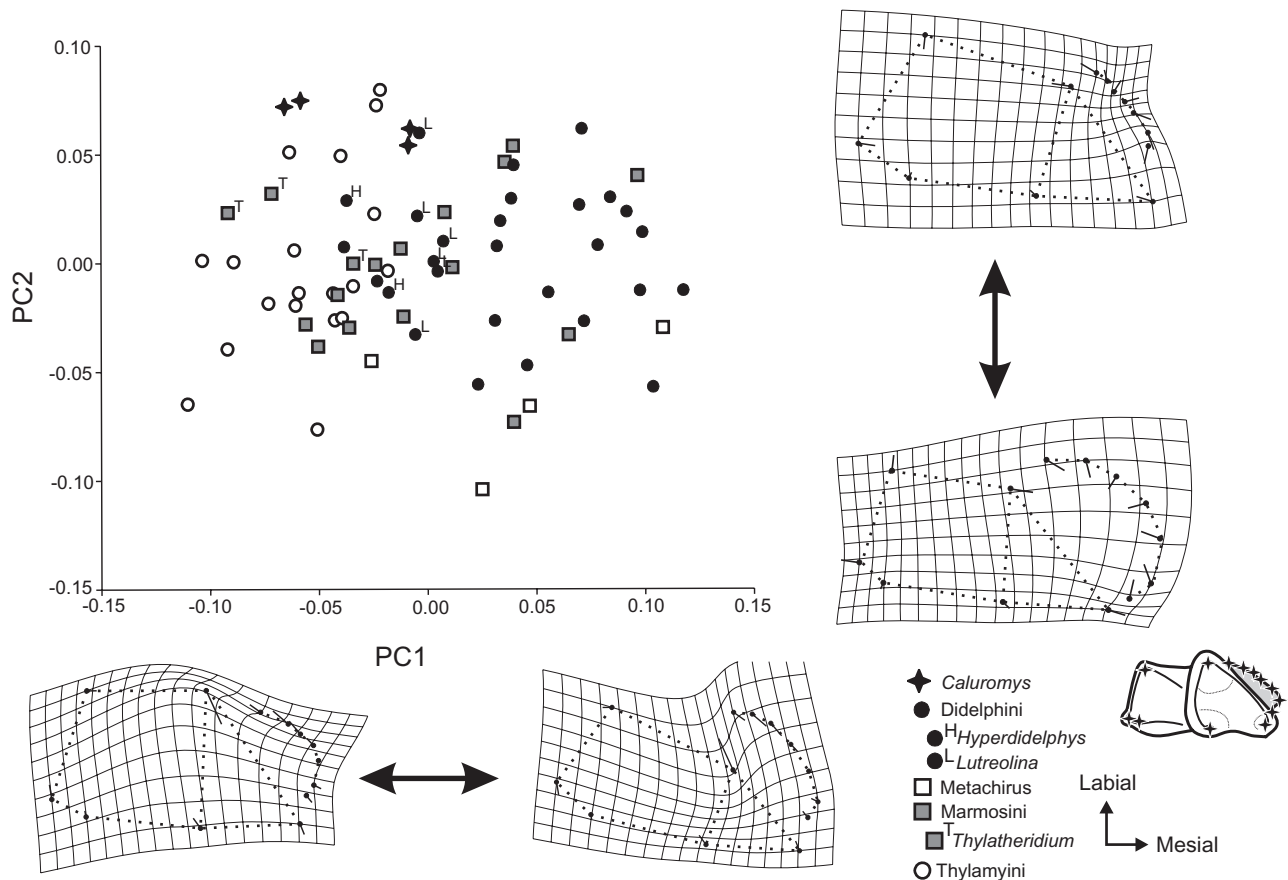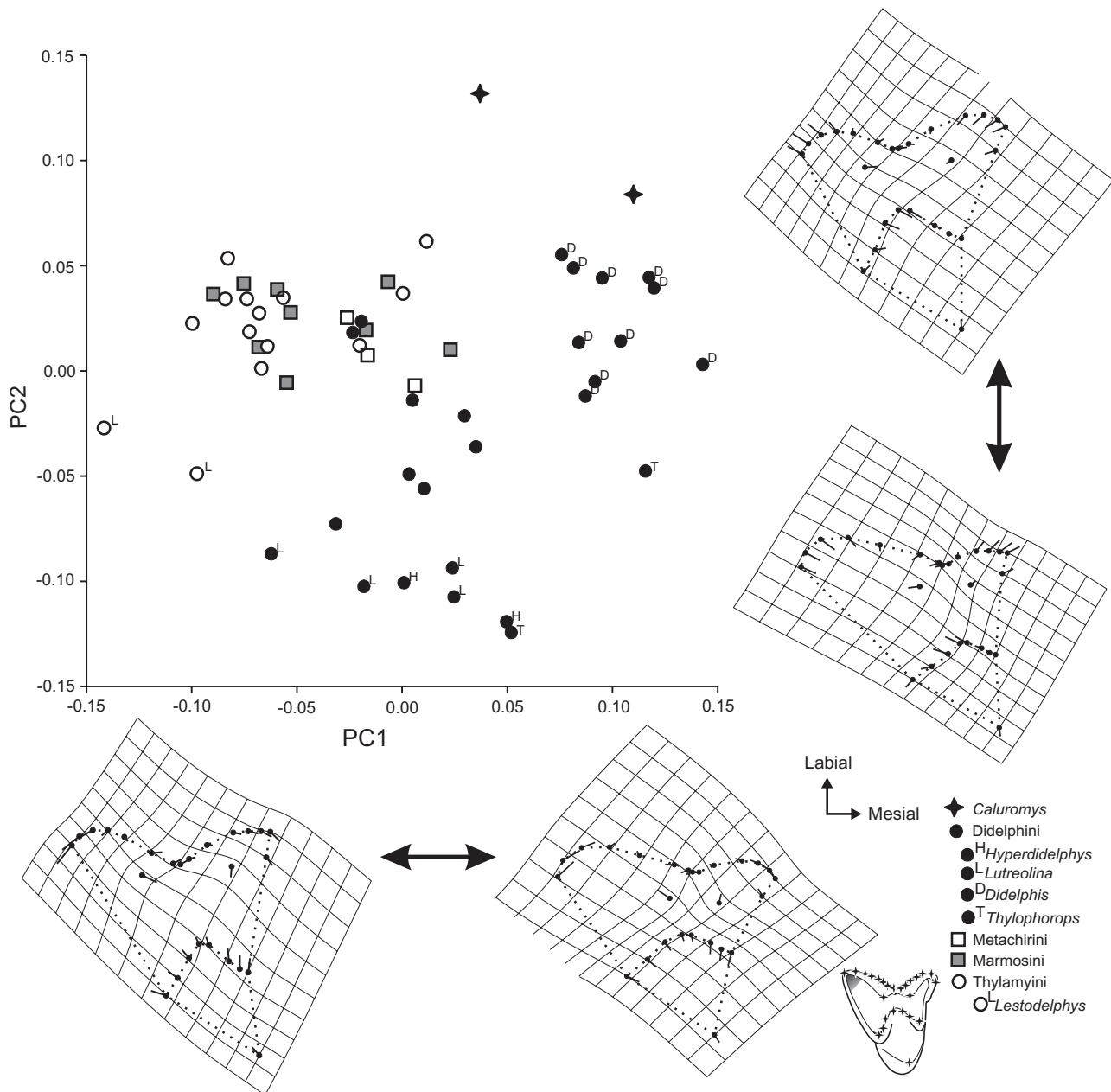
Figure 4. Third lower molar (m3) shape variation along the first two principal components (PC) from the PCA of the Procrustes coordinates, showing the distribution of taxonomic groups. Deformation grids show the extreme shape of each PC.

Between-group PCA of M1 showed a better separation of diet categories (Fig. S6). Diet category I was clearly separated on the positive end of both axes (i.e. upper right quadrant of Fig. S6). The remaining categories form a continuum, with diet categories II and IV separated along PC1, and categories V and III forming a cluster separated from category IV along PC2 (Fig. S6). Variation towards the positive end of PC1 can be associated with a longer M1, a more inflected centrocrista, a shallower ectoflexus, distally displaced metacone, a narrower stylar shelf at the metastylar corner and a mesially displaced StD (Fig. S6). Variation towards the positive end of PC2 was also associated with a wider molar (labiolingually), with a shallower ectoflexus and a less inflected centrocrista, a shorter metacrista, and twinned StB and StD (Fig. S6).

The separation of diet categories obtained using the between-group PCA was better for both upper and lower third molars (i.e. m3 and M3). The plot of m3 showed a continuum among the five diet categories, with the centroid of category I located inside the ellipse of cat-

egory II, both being separated from categories V and IV along the first axis, while category III was orientated towards the positive end of the second axis (Fig. 6). Shape changes towards the positive end of PC1 included a narrower molar, smaller talonid, distally displaced paraconid and larger anterior cingulum (Fig. 6). Towards the positive end of PC2, m3 became narrower, the entoconid and hypoconulid became distolabially displaced, while the hypoconid and protoconid were mesiolingually displaced (Fig. 6). In the plot of M3, the five diet categories were clearly better separated (Fig. 7). Categories II, IV and V were separated along PC2, while categories I and III were separated from each other three along PC2 and from the other three categories along PC1 (Fig. 7). Towards the positive end of PC1, M3 became shorter and broader, molars showed a sharper centrocrista and deeper ectoflexus, a larger stylar shelf, and labially displaced StB and StD (Fig. 7). Shape changes towards the positive end of PC2 included the labial displacement of StA, mesial displacement of StE, labial displacement of StB and StD, along with a separation of both cusps from each other, lingual

Figure 5. Third upper molar (M3) shape variation along the first two principal components (PC) from the PCA of the Procrustes coordinates, showing the distribution of taxonomic groups. Deformation grids show the extreme shape of each PC.

displacement of the paracone, metacone and protocone, and a more inflected ectoflexus and centrocrista (Fig. 7).

SHAPE CHANGES ALONG PHYLOGENY

The optimization of M3 showed changes both on the terminal taxa and on the internal nodes, being more important on the former (Fig. S7). The node that groups all Didelphinae (node 1, Fig. 8) showed displacement

on most of the landmarks from the root pattern (i.e. *Caluromys*), the main changes being the shortening of the molar, the lengthening of the metacrista caused by a mesial displacement of the metacone and a labial displacement of StE, a reduction of the anterior cingulum evidenced by the posterior displacement of landmark 15, and mesial displacement of the protocone. The terminal node of *Monodelphis* showed a larger stylar shelf, a less inflected centrocrista, labial
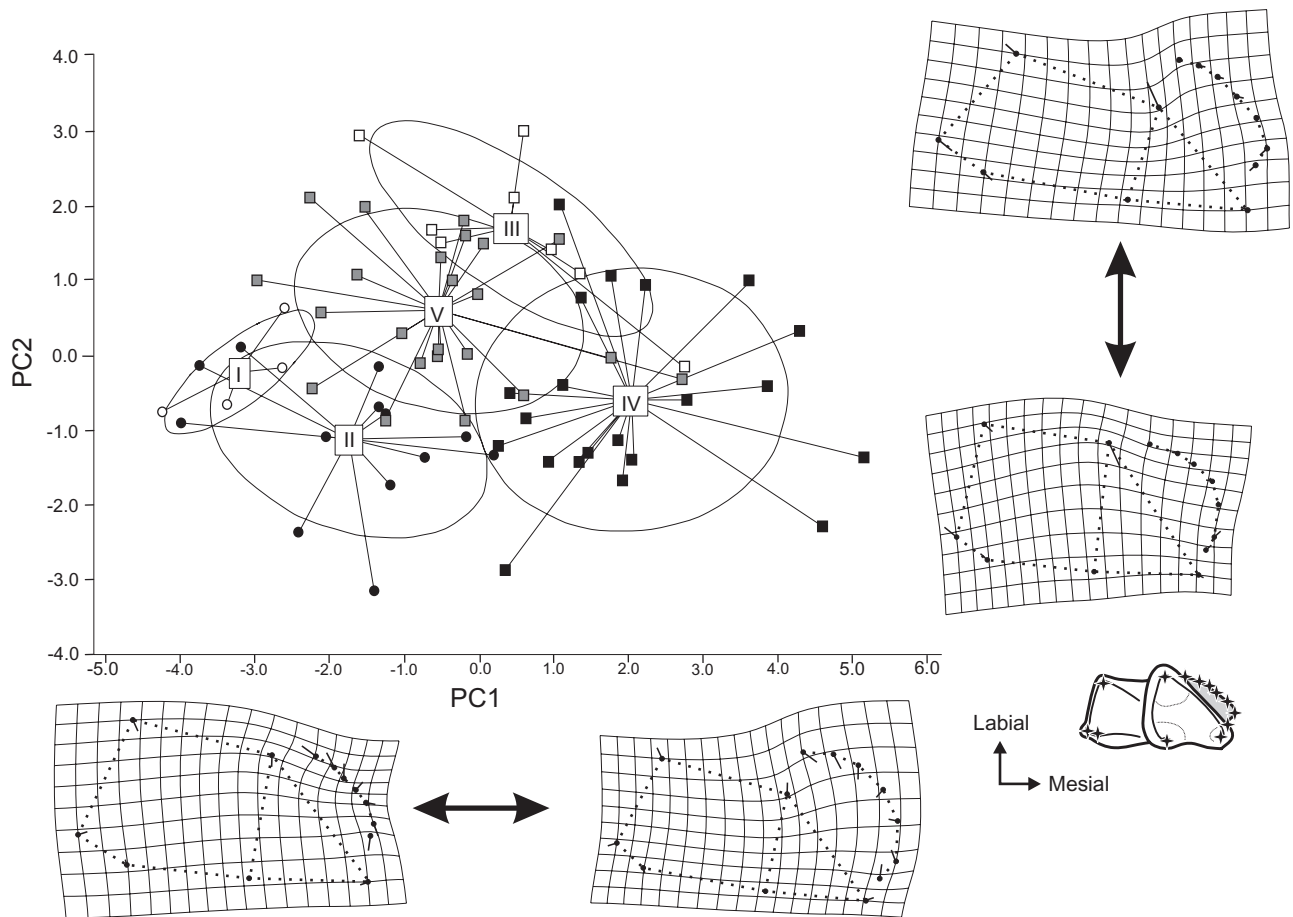
Figure 6. Scatter plots resulting from the between-group PCA of the third lower molar (m3), summarizing differences between the five diet categories. White squares with the Roman numeral of each diet category represent the centroid of the distribution for that category. Deformation grids show the extreme shape of each PC.

displacement of the protocone, distal displacement of the metacone and StD, and mesial displacement of StB (Fig. 8). The node that groups tribe Thylamyini showed a longer metacrista and a deeper ectoflexus (node 4, Fig. 8). The next node that showed important changes was the one that groups *Thylamys* and *Lestodelphys*, with a shortening of the molar, a distolabial displacement of StB and distolingual displacement of StD, and a deeper ectoflexus (node 6, Fig. 8). *Lestodelphys* showed a shortening of the molar, an expansion of the stylar shelf (mainly at the metastylar corner), a lingually displaced protocone and a less inflected centrocrista; in *Thylamys* StB and StD were lingually displaced (Fig. 8). The lingual displacement of StB and StD was also observed in the node that groups Metachirini and Didelphini, and in *Metachirus* (node 8, Figs 8 and S7). *Metachirus* also showed a longer metacrista, and a labially inflected centrocrista. The node of Didelphini showed a distolabial displacement of the protocone and a less inflected centrocrista (node 10, Fig. S7). *Chironectes* showed a shallower ectoflexus, a shorten-

ing of the metacrista, a mesial displacement of StA and distal displacement of the protocone (Fig. 8). Stylar cusp E was distally displaced, and the protocone was labially displaced on the node that groups the remaining genera of Didelphini (node 10, Fig. 8). *Didelphis* showed a longer molar, with a shorter metacrista, a smaller stylar shelf and a less inflected centrocrista (Fig. 8). A less inflected ectoflexus and mesial displacement of StD were observed on the node that groups *Thylophorops*†, *Lutreolina* and *Hyperdidelphys*† (node 11, Fig. 8). *Thylophorops*† showed a longer and more distally displaced metacrista, and a mesially displaced protocone (Fig. 8). *Hyperdidelphys*† showed a similar pattern, but with a narrower stylar shelf, a distally displaced StA and anterior cingulum, and a lingually displaced protocone (Fig. 8). *Lutreolina* showed a shorter molar, with a less inflected centrocrista, a poorly developed ectoflexus, a distolabially displaced StD and a labially displaced protocone (Fig. 8). The optimization of M1 shows a similar pattern, but changes are more subtle in most specimens analysed (Fig. S8).
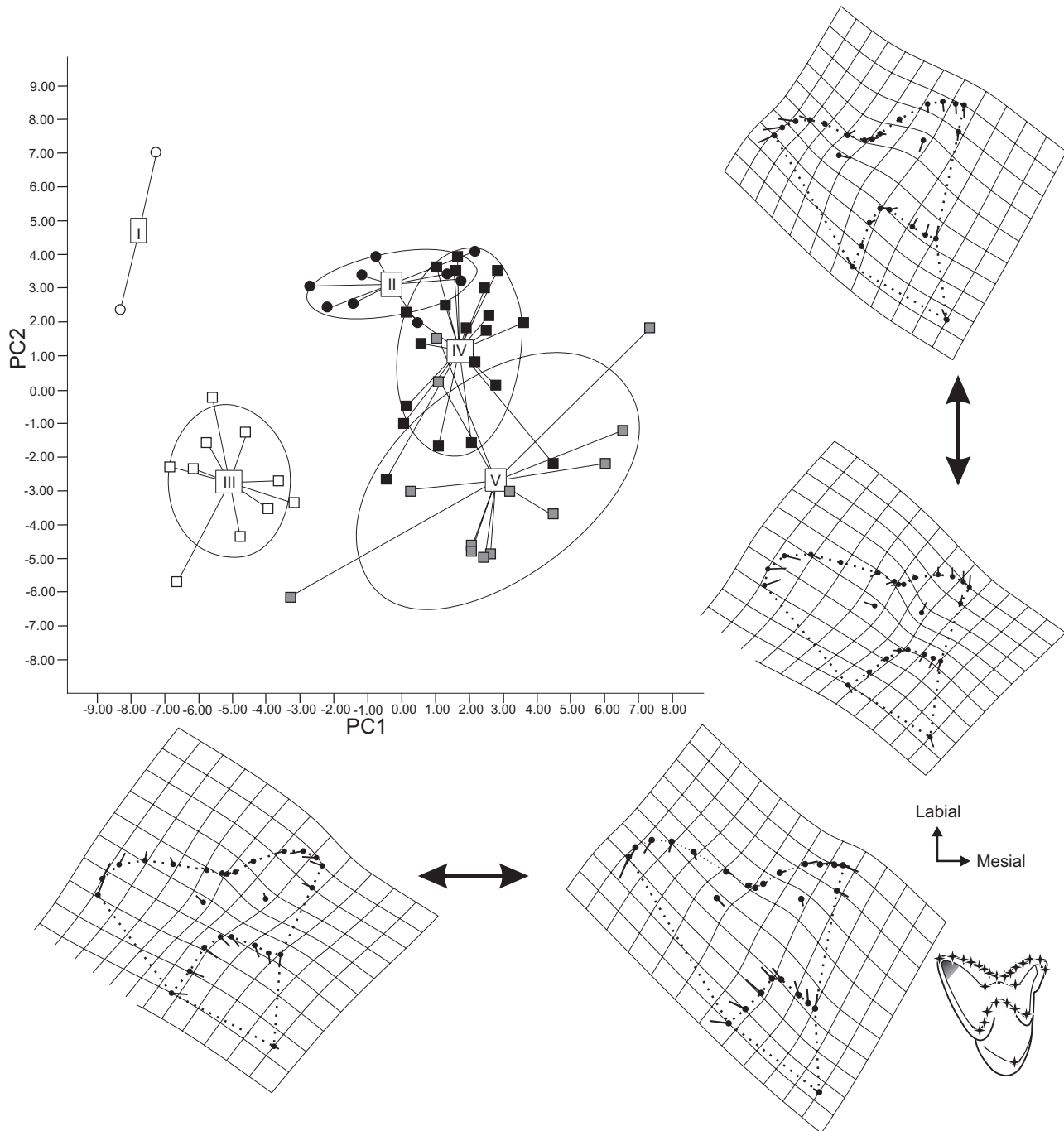
Figure 7. Scatter plots resulting from the between-group PCA of the third upper molar (M3), summarizing differences between the five diet categories. White squares with the Roman numeral of each diet category represent the centroid of the distribution for that category. Deformation grids show the extreme shape of each PC.

The optimization of m3 also showed more changes on the terminal taxa than on the internal nodes (Fig. S9). The Didelphinae node showed a labial displacement of the entoconid, a mesial displacement of the hypoconulid, a lingual displacement of the protoconid and a larger anterior cingulum (node 1, Fig. 9). Inside

tribe Marmosini, the node that groups *Thylatheridium*†and *Monodelphis* showed a lingual displacement of the hypoconid and a distolabial displacement of the metaconid (node 3, Fig. 9), while in *Thylatheridium*†there was an enlargement of the trigonid, and in *Monodelphis* the entoconid and the hypoconulid were
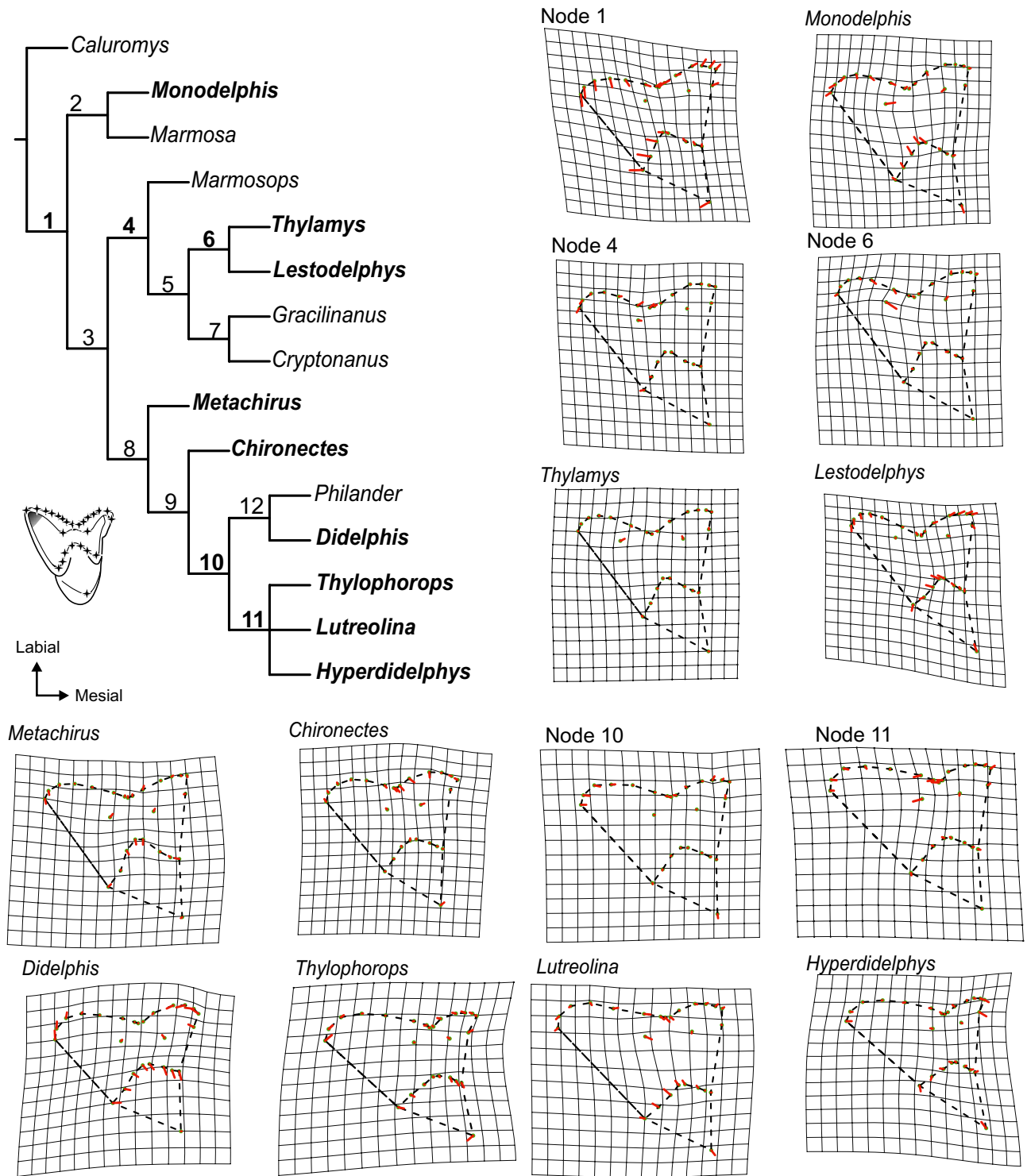
Figure 8. Phylogeny showing a summary of the optimization for the third upper molar (M3). Numbers on the branches indicate node number. Taxon names and nodes in bold indicate the optimizations being shown. Deformation grids show the changes with respect to the previous node.
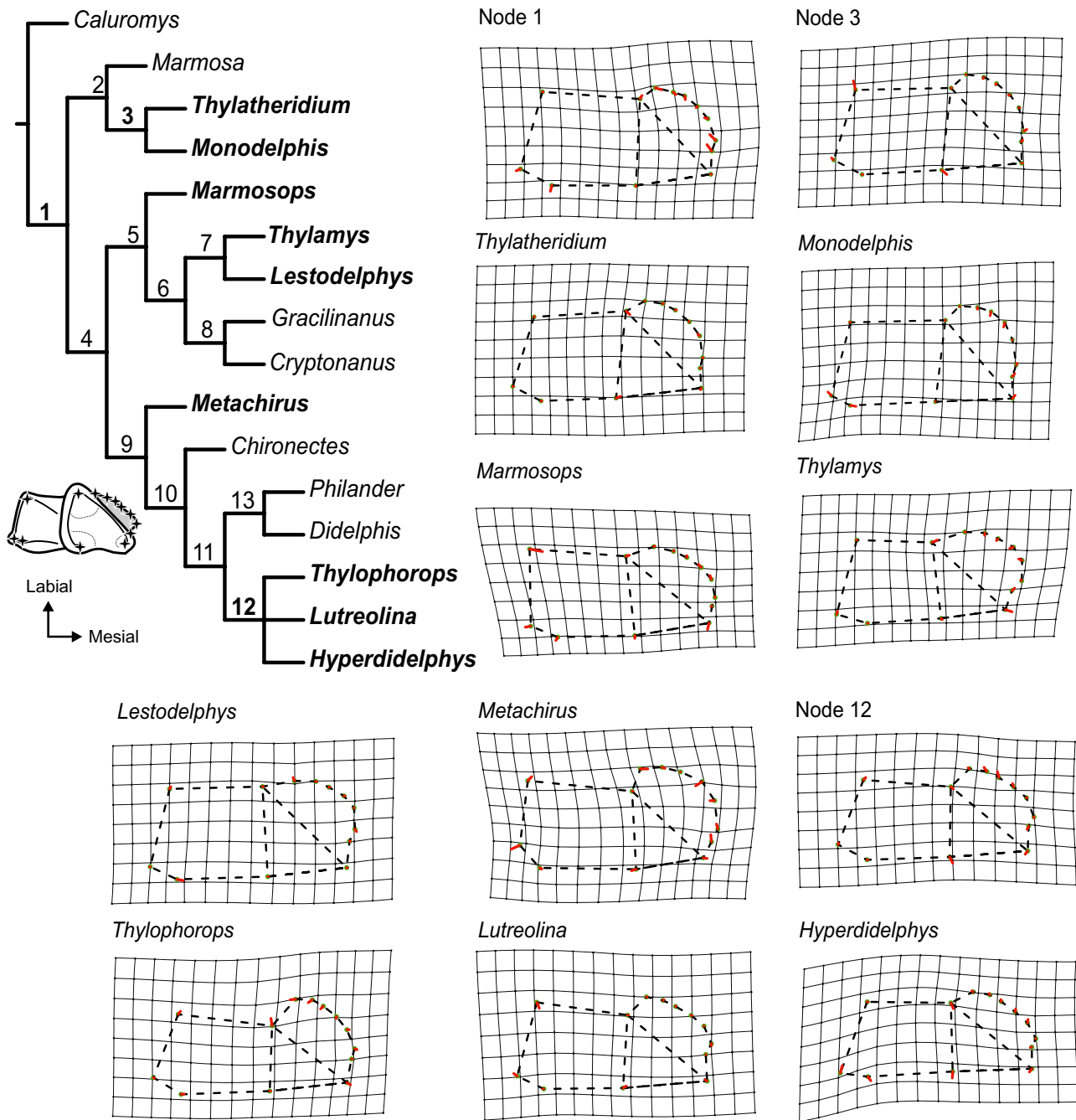
Figure 9. Phylogeny showing a summary of the optimization for the third lower molar (m3). Numbers on the branches indicate node number. Taxon names and nodes in bold indicate the optimizations being shown. Deformation grids show the changes with respect to the previous node.

twinned, the paraconid was distolingually displaced and the anterior cingulum was larger (Fig. 9). Within tribe Thylamyini, the main changes are on the terminal taxa, while the basal node showed only a distolabial displacement of the protoconid, and a labial displacement of the metaconid (node 5, Fig. S9). *Marmosops* showed a distally displaced hypoconid, a labially dis-

placed paraconid, metaconid and entoconid and a mesially displaced hypoconulid (Fig. 9). *Thylamys* showed a smaller trigonid with a distally displaced paraconid and protoconid, and a larger anterior cingulum (Fig. 9). *Lestodelphys* showed a distally displaced entoconid (Fig. 9), while *Gracilinanus* Gardner & Creighton showed a mesiolingual displacement of the protoconid

Table 2. Results of the redundancy analyses of molar morphology, diet size and phylogeny

	m1		M1		m3		M3	
	%	*P*	%	*P*	%	*P*	%	*P*
Total	72.71	0.2272	81.75	**0.0041**	85.71	**0.0004**	85.53	**0.0002**
Diet	15.09	**0.0176**	21.51	**0.0001**	9.68	0.0705	20.3	**0.0005**
Diet partial var.	6.02	0.9331	5.97	0.1593	3.5	0.4608	4.77	0.3154
Size	10.73	**0.0037**	10.83	0.0713	13.35	**0.0347**	25.01	**0.0003**
Size partial var.	3.67	0.5115	4.51	0.3299	4.9	0.3622	4.78	0.3757
Phylogeny	62.09	**0.0261**	72.42	**0.006**	76.19	**0.0001**	74.25	**0.0001**
Phylogeny partial var.	48.19	0.5758	47.58	0.0764	64.68	**0.0022**	40.15	**0.0034**

%, percentage of variance explained by each analysis; *P*, probability for each analysis (bold numbers are significant at $P < 0.05$); partial var, partial variance explained by one factor (e.g. diet) but not by the others (i.e. size, phylogeny).

and metaconid, a mesial displacement of the paraconid, a lingual displacement of the entoconid, a distal displacement of the hypoconulid, a labial displacement of the hypoconid and a smaller anterior cingulum (Fig. S9). The anterior cingulum became larger in *Metachirus*, the metaconid and hypoconulid were mesially displaced, the hypoconid was distolingually displaced and the paraconid was distally displaced (Fig. 9). The basal node of Didelphini showed only a mesial displacement of the hypoconid (node 10, Fig. S9). *Chironectes* showed a longer talonid with a labially displaced hypoconid, and a shorter trigonid with a lingually displaced protoconid, paraconid and metaconid, the displacement being much larger on the protoconid, and a larger anterior cingulum (Fig. S9). The node that groups *Philander* and *Didelphis* showed a mesiolingual displacement of the protoconid (node 13, Fig. S9). The node that groups *Lutreolina*, *Thylophorops*† and *Hyperdidelphys*† showed a labial displacement of the metaconid, a mesiolabial displacement of the paraconid, a distolabial displacement of the protoconid, a distolingual displacement of the hypoconid and a smaller anterior cingulum (node 12, Fig. 9). In *Thylophorops*† the protoconid was lingually displaced, the paraconid distolabially displaced, the hypoconid distolingually displaced and the anterior cinugulum was larger (Fig. 9). *Lutreolina* showed a labially displaced hypoconid, a mesiolingually displaced hypoconulid and a distally displaced metaconid (Fig. 9). *Hyperdidelphys*† showed a labial displacement of the metaconid and protoconid, a mesiolabial displacement of the paraconid, a distolingual displacement of the hypoconulid, and a distolabial displacement of the entoconid (Fig. 9). The optimization of m1 showed similar changes (Fig. S10).

CORRELATION BETWEEN MORPHOLOGY, PHYLOGENY, SIZE AND ECOLOGY

For all molars, the final model chosen by AIC omitted four nodes of the phylogeny: node 2 in all four molars,

node 13 in M1, node 12 in lower molars and M3, nodes 7 and 3 in M3, and nodes 8 and 4 in lower molars and M1 (see Figs 8, 9, S8–S10 for node numbers). The model using three factors as constraints (diet, size and phylogeny) explained between 72.71 and 85.71% of the total shape variation (Table 2). Diet explained between 9.68 and 21.51% of the variance in all molars, while the proportion explained exclusively by this variable was much lower and statistically not significant (Table 2). Centroid size accounted for 3.67–4.9% of the total variation when using the remaining factors as conditioning matrix, and 10.73–25.01%, when using size as a constraint (Table 2). Finally, phylogeny explained between 62.09 and 76.19% of the variation, although it explained only between 40.15 and 64.68% of the shape variation by itself (Table 2).

DISCUSSION

Because teeth are the principal structure involved in the mechanical breakdown of food in mammals, the morphology of cusps and crests in occlusal view should be expected to show different levels of correlation with diet (e.g. Kay & Sheine, 1979; Strait, 1993; Evans, 2005; Evans & Sanson, 2006; Evans *et al*., 2007; Hogue & ZiaShakeri, 2010). Surprisingly, our results seem to contradict this premise, as we found low correlation between molar shape and diet. The PCA of the Procrustes coordinates of the four molars showed a broad superposition of diet categories, except category I (represented only by the genus *Caluromys*), which showed a trend separating it from the remaining diet categories (Figs 2–5). By using a BG-PCA, which maximizes the separation between the centroids (or means) of the different groups without distorting the shape distances (Mitteroecker & Bookstein, 2011; Seetah *et al*., 2012), we obtained a better separation of the diet categories in third molars; however, there was overlap of all categories in m3, and categories II, IV and V in

M3 (Figs 6, 7). Even some specimens of category IV were placed near the centroid of the distribution of category V and vice versa in M3 (Fig. 7). In the between-group analysis of first lower and upper molars, we did not observe a better separation in the distribution of diet categories. Most of them overlapped and even the centroids of some categories were placed inside the confidence ellipses of the other categories (Figs S5, S6). Such differences in fitting tooth shape variation to any diet category are expected, because in adult marsupials with permanent dentition, the last molars (M3, m3–m4) are placed in an optimal place from a biomechanical view (see Werdelin, 1987). Consequently, we expect a better correlation between these molars and diet than between anterior molars and diet.

There are many factors that could be obscuring the relationship between molar shape and diet. Didelphid marsupials have primitive tribosphenic molars, which due to their generalized shape are flexible and allow the consumption of different kinds of food (Goin *et al*., 1992). This is reflected in their dietary flexibility, with the main items consumed by this group of marsupials being a mix of small vertebrates, arthropods, fruits and nectar in different proportions (Vieira & Astúa de Moraes, 2003; Ungar, 2010). In fact, the diet classification used in this contribution showed a continuum from mostly frugivorous to mainly carnivorous species, where none of the neotropical marsupials fed exclusively on plant material, invertebrates or vertebrates (Vieira & Astúa de Moraes, 2003). For example, one of the most carnivorous species of the group, *Lestodelphys halli*, does not feed exclusively on vertebrates, but also consumes insects (Martin, 2008), which can be an important item in their diet in some localities (Zapata *et al*., 2013). As this is a small species (total length less than 250 mm, mass 60–90 g; Pearson, 2007), it is possible that diet would shift seasonally depending on prey availability and/or with age, with younger individuals consuming more arthropods and older ones being active rodent hunters (Martin & Udrizar Sauthier, 2011). Arthropods, as well as leaves, have a high proportion of structural carbohydrates in their composition, which are usually difficult to digest and need to be ground into smaller pieces for easier digestion (Kay & Sheine, 1979). Consequently, the consumption of arthropods might create a structural constraint that the shape of the molars is more in accordance with an insect-based diet than with a meat based one, even when the first item is not an important item in the diet of this marsupial. Species specialized in eating insects tend to have longer shearing crests than other species (Kay & Hylander, 1978; Kay & Sheine, 1979; Hogue & ZiaShakeri, 2010), and these crests tend to be more transverse than longitudinal with respect to the mesiodistal axis of the molar series, while in carnivorous species the crests tend to be more

parallel to that axis (Goin *et al*., 1992). The plot of M3 showed a clear example of the constraint caused by the most demanding food item in *Lestodelphys* (demanding in the sense of the functional requirements needed to process the food item), as this species is placed on the negative end of PC1, having a long metacrista transverse to the mesiodistal axis of the tooth row (Fig. 5). By contrast, taxa that consume (or are thought to consume) a much smaller proportion of invertebrates, such as *Lutreolina*, *Hyperdidelphys*† and *Thylophorops*†, were placed on the negative end of PC2, with the metacrista more parallel to the mesiodistal axis of the tooth row (Fig. 5). Hogue & ZiaShakeri (2010) also found inconsistencies between the length of molar crests and the proportion of insects or leaves eaten by a broader group of marsupials. Similarly to what happens with *Lestodelphys*, they found that carnivorous species that consume even a small proportion of insects have long shearing crests in m3, characteristic of insectivorous species. Thus, the absence of a better correlation between diet and molar shape could be related to the absence of highly specialized species, and the need for retaining a shape that can be useful to process different kinds of food items. In this context, the basic pattern of a tribosphenic molar appears to be the best morphology when coping with mixed diets. This does not mean that New World marsupials are not subject to adaptive pressures (with a subsequent diversion from the generalized pattern), but implies that the generalized tribosphenic molar morphology occurring in these species represents the best solution to different diets, working effectively for most species with only minor deviations to reflect changes in the main diet preferences. Therefore, small changes in morphology would be represented by minor differences in, for example, the orientation and length of the metacrista, the relationship between protocone/talonid size, trigonid–talonid proportions and length of the cristid obliqua. Our placing of the studied genera in the feeding categories we used allowed us to assess those differences, despite them being relatively small.

Another possible explanation for the weak relationship between molar shape and diet could be a recent radiation of the group, where the ecological specialization occurred faster than the morphological changes. However, Meredith *et al*. (2008) estimated a date of approximately 40 Mya for the splitting of Didelphinae from *Caluromys*, and 30 Mya for the splitting of *Monodelphis* from the remaining Didelphinae. Thus, we believe that the morphological uniformity of the molars is unlikely to be attributable to a recent radiation of the group.

One important factor to take into account when analysing our results is the impact of the phylogenetic legacy. The canonical phylogenetic analyses showed that in all analysed molars, phylogeny alone (without taking

into account the interaction with other variables) explained between 40 and 65% of the variance, while diet never explained more than 6% (the model was never statistically significant, compared with phylogeny which was significant for the third molars). Without excluding the interaction between variables, the percentage of variance explained by diet rises to 10–20%, but the percentage explained by the phylogeny also increases, rising to 62–72%. Thus, at least half of the shape variance explained by diet is related to phylogenetic relationships, meaning that only a small part of the molar shape was influenced by diet during evolution of the group. An example of this effect of phylogenetic legacy can be found in the similar molar shape described for *Lestodelphys* and *Thylamys* despite some differences in diet. The same trend was observed with allometry, which could be interpreted as a structural constraint (Hall, 1999). The largest proportion of the molar shape is exclusively related to the position of each genus on the phylogenetic tree, which is difficult to explain given that phylogeny is not an evolutionary constraint but rather the pattern of evolutionary change over time, or the correlation of cladogenetic events and morphological patterns (Losos, 2011). What is usually termed phylogenetic constraint or phylogenetic inertia is related to restrictions on the evolutionary trajectories imposed by previous adaptations (Johnson, McKinney & Sorenson, 1999), and includes several genetic, developmental and fitness constraints on evolution, which is ultimately related to natural selection (Shanahan, 2011). In our results, we found a strong phylogenetic effect (meaning a slow rate of character evolution related to the rate of cladogenesis; Losos, 2011), but the data available make the real constraints behind this historical pattern difficult to distinguish. We believe that the broad ecological niche used by most of the groups/genera studied herein (at least regarding diet) did not generate enough selective pressure on molar morphology to override pre-existing differences that occur among clades, subsequently confounding the relationship between diet and tooth shape. Additionally, because a large proportion of shape variation is related to phylogeny and not to size or diet, it is possible that this part of the variation is related to genetic drift, which could be translated on a macroevolutionary scale to an evolutionary model similar to a random walk or Brownian motion or other models where the change occurred at speciation (Felsenstein, 1985).

The molar shape optimization analysis on phylogeny reinforces the ideas mentioned above. When analysing the optimization of M3 in some key taxa, such as representatives of the most carnivorous category (V), it can be seen how the length and position of the metacrista (one of the main indicators of the carnivorous diet) is influenced by the position of taxa in the phylogeny (Figs 8 and S7). The clade formed by *Lutreolina*, *Thylophorops*† and *Hyperdidelphys*† (all carnivores) show long metacristae, more longitudinally orientated to the mesiodistal axis of the tooth row, while *Lestodelphys*, which is placed in a distant node with the insectivorous genus *Thylamys*, shows the metacrista orientated more transverse to the mesiodistal axis of the tooth row, a change of shape also present in the optimization of the node of that clade (node 6, Fig. 8). Something similar can be observed in the optimization of m3, where the length and orientation of the paracristid follows the same pattern as the metacrista. In the analysis of m3 we also included representatives of the carnivorous genus *Thylatheridium*†, which is the sister group to the insectivorous/carnivorous genus *Monodelphis*. The optimization of *Thylatheridium*† showed a long transversely orientated paracristid, a feature more related to insectivory than to carnivory (Fig. 9). Consequently, the dental morphology exhibited by the ancestor of each taxon clearly influences dental shape, causing species with similar diets to have different molar shapes.

In some cases, we also observed convergent shapes as a solution to similar diet constraints. For example, the PCA of M1 showed several carnivorous species from different phylogenetic lineages grouped in the lower right quadrant of the graph (Figs 3 and S2), consequently exhibiting similar molar shapes. This convergence was also observed in the optimization of M1 and M3 in the phylogeny, where a larger stylar shelf, mainly at the metastylar corner, was observed independently in several carnivorous/faunivorous genera: *Lestodelphys*, *Monodelphis* and the clade *Thylophorops*† + *Lutreolina* + *Hyperdidelphys*† (Fig. S7). What remains to be tested is the shape optimization of the molars of *Caluromys*, a group placed on the other end of the diet variation, being mostly frugivorous. Future analyses including taxa placed outside Didelphidae will help to describe the evolutionary history of the molar shape of a group that shows such a distinctive morphology (at least as seen in our results).

The constraints posed to the molar shape by the phylogenetic legacy have been described previously by many authors in other mammal groups (e.g. Kay & Hylander, 1978; Strait, 1993) and even in marsupials (Hogue & ZiaShakeri, 2010). However, this is the first study to clearly show the bias caused by the phylogenetic legacy using new methodologies to reconstruct the ancestral shape of the molars throughout the phylogeny of the group. The pattern observed in the reconstruction of the ancestral shapes reinforces the results of the canonical phylogenetic analysis, which showed that most of the molar shape variance was explained by phylogeny, while diet category and size explained only a small proportion of that variance.

Nonetheless, it is important to keep in mind that the tribosphenic molar is very versatile, and allowed members of the Didelphidae to develop different diets (although the differences might not be as strong as in other groups of mammals) without the need for dramatic shape change in the molars.

In summary, the analyses here indicated a weak relationship between molar shape and diet. On the one hand, this could be related to the lack of strong dietary specializations, where maintaining a molar able to cope with mixed diets is highly advantageous. On the other hand, the strong correlation found between the position of the taxa on the phylogeny and molar shape indicates that the shape exhibited by each taxon is highly influenced by phylogenetic legacy. This was clearly seen in the optimizations, where although some convergences were observed, we also found that taxa with similar diets showed molars with different shapes, with a strong influence of the shape of sister taxa.

ACKNOWLEDGEMENTS

REFERENCES

Abello MA, Ortiz Jaureguizar E, Candela AM. 2012. Paleoecology of the Paucituberculata and Microbiotheria (Mammalia, Marsupialia) from the late Early Miocene of Patagonia. In: Vizcaíno SF, Kay RF, Bargo S, eds. *Early Miocene Paleobiology in Patagonia: high-latitude paleocommunities of the Santa Cruz Formation*. Cambridge: Cambridge University Press, 156–172.

Archibald JD, Averianov AO. 2012. Phylogenetic analysis, taxonomic revision, and dental ontogeny of the Cretaceous Zhelestidae (Mammalia: Eutheria). *Zoological Journal of the Linnean Society* **164:** 361–426.

Bookstein FL. 1997. Landmark methods for forms without landmarks: morphometrics of group differences in outline shape. *Medical Image Analysis* **1:** 225–243.

Case JA, Goin FJ, Woodburne MO. 2005. 'South American' marsupials from the Late Cretaceous of North America and the origin of marsupial cohorts. *Journal of Mammalian Evolution* **12:** 461–494.

Catalano SA, Giannini N, Goloboff PA. 2010. Phylogenetic morphometrics (I): the use of landmark data in a phylogenetic framework. *Cladistics* **26:** 539–549.

Catalano SA, Goloboff PA. 2012. Simultaneously mapping and superimposing landmark configurations with parsimony as optimality criterion. *Systematic Biology* **61:** 392–400.

Caumul R, Polly PD. 2005. Phylogenetic and environmental components of morphological variation: skull, mandible, and molar shape in marmots (*Marmota*, Rodentia). *Evolution* **59:** 2460–2472.

Crompton AW, Hiiemae KM. 1969. Functional occlusion in tribosphenic molars. *Nature* **222:** 678–679.

Crompton AW, Hiiemae KM. 1970. Molar occlusion and mandibular movements during occlusion in the American opossum, *Didelphis marsupialis* L. *Zoological Journal of the Linnean Society* **49:** 21–47.

Dray S, Dufour AB. 2007. The ade4 package: implementing the duality diagram for ecologists. *Journal of Statistical Software* **22:** 1–20.

Dumont ER, Strait SG, Friscia AR. 2000. Abderitid marsupials from the Miocene of Patagonia: an assessment of form, function, and evolution. *Journal of Paleontology* **74:** 1161–1172.

Evans AR. 2005. Connecting morphology, function and tooth wear in microchiropterans. *Biological Journal of the Linnean Society* **85:** 81–96.

Evans AR, Sanson GD. 2006. Spatial and functional modeling of Carnivore and Insectivore molariform teeth. *Journal of Morphology* **267:** 649–662.

Evans AR, Wilson GP, Fortelius M, Jernvall J. 2007. High-level similarity of dentitions in carnivorans and rodents. *Nature* **445:** 78–81.

Felsenstein J. 1985. Phylogenies and the comparative method. *American Naturalist* **125:** 1–15.

Fox RC. 1987. Palaeontology and the early evolution of marsupials. In: **Archer M, ed.** *Possums and opossums: studies in evolution*, *Vol. 1*. Sydney: Surrey Beatty & Sons, 161–169.

Giannini NP. 2003. Canonical Phylogenetic Ordination. *Systematic Biology* **52:** 684–695.

Godínez-Domínguez E, Freire J. 2003. Information-theoretic approach for selection of spatial and temporal models of community organization. *Marine Ecology Progress Series* **253:** 17–24.

Goin FJ, Montalvo CI. 1988. Revisión sistemática y reconocimiento de una nueva especie del género *Thylatheridium* Reig (Marsupialia, Didelphidae). *Ameghiniana* **25:** 161–167.

Goin FJ, Pardiñas UFJ. 1996. Revisión de las especies del Género *Hyperdidelphys* Ameghino, 1904 (Mammalia, Marsupialia, Didelphidae). Su significación filogenética, estratigráfica y adaptativa en el Neógeno del Cono Sur Sudamericano. *Estudios Geológicos* **52:** 327–359.

Goin FJ, Velázquez C, Scaglia O. 1992. Orientación de las crestas cortantes en el molar tribosfénico. Sus implicancias funcionales en didelfoideos (Marsupialia) fósiles y vivientes. *Revista del Museo de La Plata (Nueva Serie)* **9:** 183–198.

Goloboff PA, Catalano SA. 2011. Phylogenetic morphometrics (II): algorithms for landmark optimization. *Cladistics* **27:** 42–51.

Goloboff PA, Farris J, Nixon K. 2008. TNT, a free program for phylogenetic analysis. *Cladistics* **24:** 774–786.

Hall BK. 1999. *Evolutionary developmental biology*. Dordrecht: Kluwer Academic Publishers.

Hillson S. 2005. *Teeth, 2nd edn*. Cambridge: Cambridge University Press.

Hogue AS, ZiaShakeri S. 2010. Molar crests and body mass as dietary indicators in marsupials. *Australian Journal of Zoology* **58:** 56–68.

Johnson KP, McKinney F, Sorenson MD. 1999. Phylogenetic constraint on male parental care in the dabbling ducks. *Proceedings of the Royal Society London B* **266:** 759–763.

Kay RF. 1975. The functional adaptions of primate molar teeth. *American Journal of Physical Anthropology* **43:** 195–216.

Kay RF, Hylander WL. 1978. The dental structure of mammalian folivores with special reference to primates and Phalangeroidea (Marsupialia). In: Montgomery GG, ed. *The ecology of arboreal folivores*. Washington, DC: Smithsonian Institute Press, 173–191.

Kay RF, Sheine WS. 1979. On the relationship between chitin particle size and digestibility in the primate *Galago senegalensis*. *American Journal of Physical Anthropology* **50:** 301–308.

Klingenberg CP. 2011. MorphoJ: an integrated software package for geometric morphometrics. *Molecular Ecology Resources* **11:** 353–357.

Klukkert ZS, Teaford MF, Ungar PS. 2012. A dental topographic analysis of chimpanzees. *American Journal of Physical Anthropology* **148:** 276–284.

Legendre P, Legendre L. 1998. *Numerical ecology, 2nd edn*. Amsterdam: Elsevier.

Losos JB. 2011. Seeing the forest for the trees: the limitations of phylogenies in comparative biology. *American Naturalist* **177:** 709–727.

Luo ZX, Cifelli RL, Kielan–Jaworowska Z. 2001. Dual origin of tribosphenic mammals. *Nature* **409:** 53–57.

Martin GM. 2005. Intraspecific variation in *Lestodelphys halli* (Marsupialia: Didelphimorphia). *Journal of Mammalogy* **86:** 793–802.

Martin GM. 2008. *Sistemática, distribución y adaptaciones de los marsupiales patagónicos*. Unpublished Doctoral Thesis, Facultad de Ciencias Naturales y Museo, Universidad Nacional de La Plata.

Martin GM, Udrizar Sauthier DE. 2011. Observations on the captive behavior of the rare Patagonian opossum *Lestodelphys halli* (Thomas, 1921) (Marsupialia, Didelphimorphia, Didelphidae). *Mammalia* **75:** 281–286.

Meléndez BM. 1990. *Paleontología, tomo 3, vol 1 Mamíferos (1ª parte)*. Madrid: Paraninfo.

Meredith RW, Westerman M, Case JA, Springer MS. 2008. A phylogeny and timescale for marsupial evolution based on sequences for five nuclear genes. *Journal of Mammalian Evolution* **15:** 1–36.

Mitteroecker P, Bookstein FL. 2011. Linear discrimination, ordination, and the visualization of selection gradients in modern morphometrics. *Evolutionary Biology* **38:** 100–114.

O'Leary MA, Bloch JI, Flynn JJ, Gaudin TJ, Giallombardo A, Giannini NP, Goldberg SL, Kraatz BP, Luo Z, Meng J, Ni X, Novacek MJ, Perini FA, Zachary S. Randall ZS, Rougier GW, Sargis EJ, Silcox MT, Simmons NB, Spaulding M, Velazco PM, Weksler M, Wible1 JR, Cirranello AL. 2013. The placental mammal ancestor and the post-K–Pg radiation of placentals. *Science* **339:** 662–667.

O'Leary MA, Geisler JH. 1999. The position of Cetacea within Mammalia: phylogenetic analysis of morphological data from extinct and extant taxa. *Systematic Biology* **48:** 455–490.

Oksanen J, Blanchet FG, Kindt R, Legendre P, Minchin P, O'Hara B, Simpson GL, Solymos P, Henry M, Stevens H, Wagner H. 2013. *vegan: Community ecology package R package vers 20-6*. Available at: http://cran.r-project.org/. Accessed 28 February 2013.

Pearson OP. 2007. Genus *Lestodelphys*. In: Gardner AL, ed. *Mammals of South America, vol 1. Marsupials, xenarthrans, shrews and bats*. Chicago: The University of Chicago Press, 50–51.

Pine RH, Dalby PL, Matson JO. 1985. Ecology, postnatal development, morphometrics, and taxonomic status of the short-tailed opossum, *Monodelphis dimidiata*, an apparently semelparous annual marsupial. *Annals of Carnegie Museum* **54:** 195–231.

Prevosti FJ. 2010. Phylogeny of the large extinct South American canids (Mammalia, Carnivora, Canidae) using a 'total evidence' approach. *Cladistics* **26:** 456–481.

R Development Core Team. 2012. *R: a language and environment for statistical computing. R Foundation for Statistical Computing, Vienna*. Available at: http://wwwR-projectorg. Accessed 28 February 2013.

Reig OA, Kirsch JAW, Marshall LG. 1987. Systematic relationships of the living and neocenozoic American 'opossum-like' marsupials (suborder Didelphimorphia), with comments on the classification of these and the Cretaceous and Paleogene New World and European Metatherians. In: Archer M, ed. *Possums and opossums: studies in evolution*. Chipping Norton: Surrey Beatty and the Royal Zoological Society of New South Wales, 1–89.

Rohlf FJ. 2008a. *TpsDig, ver 2.12*. Stony Brook: Department of Ecology and Evolution, State University of New York at Stony Brook.

Rohlf FJ. 2008b. *TpsRelw, ver 1.46*. Stony Brook: Department of Ecology and Evolution, State University of New York at Stony Brook.

Seetah TK, Cardini A, Miracle PT. 2012. Can morphospace shed light on cave bear spatial–temporal variation? Population dynamics of *Ursus spelaeus* from Romualdova pećina and Vindija (Croatia). *Journal of Archaeological Science* **39:** 500–510.

Shanahan T. 2011. Phylogenetic inertia and Darwin's higher Law. *Studies in History and Philosophy of Science* **42:** 60–68.

Sheets HD. 2003. *IMP–Integrated Morphometrics Package*. Buffalo: Department of Physics, Canisius College.

Strait SG. 1993. Molar morphology and food texture among small-bodied insectivorous mammals. *Journal of Mammalogy* **74:** 391–402.

Ungar PS. 2010. *Mammal teeth: origin, evolution, and diversity*. Baltimore: Johns Hopkins University Press.

Vieira EM, Astúa de Moraes D. 2003. Carnivory and insectivory in Neotropical marsupials. In: Jones M, Dickman C, Archer M, eds. *Predators with pouches: the biology of carnivorous marsupials*. Collingwood: CSIRO Publishing, 271–284.

Voss RS, Jansa SA. 2009. Phylogenetic relationships and classification of didelphid marsupials, an extant radiation of New World metatherian mammals. *Bulletin of the American Museum of Natural History* **322:** 1–177.

Werdelin L. 1987. Jaw geometry and molar morphology in marsupial carnivores: analysis of a constraint and its macroevolutionary consequences. *Palaeobiology* **13:** 342–350.

Zapata SC, Procopio D, Travaini A, Rodríguez A. 2013. Summer food habits of the Patagonian opossum, *Lestodelphys halli* (Thomas, 1921), in southern arid Patagonian shrubsteppes. *Gayana* **77:** 64–67.

SUPPORTING INFORMATION

Additional Supporting Information may be found in the online version of this article at the publisher's web-site:

Figure S1. First lower molar (m1) shape variation along the first two principal components from the PCA of the Procrustes coordinates, showing the distribution of diet categories. Deformation grids show the extreme shape of each PC.

Figure S2. First upper molar (M1) shape variation along the first two principal components from the PCA of the Procrustes coordinates, showing the distribution of diet categories. Deformation grids show the extreme shape of each PC.

Figure S3. Third lower molar (M1) shape variation along the first two principal components from the PCA of the Procrustes coordinates, showing the distribution of diet categories. Deformation grids show the extreme shape of each PC.

Figure S4. Third upper molar (M1) shape variation along the first two principal components from the PCA of the Procrustes coordinates, showing the distribution of diet categories. Deformation grids show the extreme shape of each PC.

Figure S5. Scatterplots resulting from the between-group PCA of the first lower molar (m1), summarizing differences between the five diet categories. White squares with the Roman numeral of each diet category represent the centroid of the distribution for that category. Deformation grids show the extreme shape of each PC.

Figure S6. Scatterplots resulting from the between-group PCA of the first upper molar (M1), summarizing differences between the five diet categories. White squares with the Roman numeral of each diet category represent the centroid of the distribution for that category. Deformation grids show the extreme shape of each PC.

Figure S7. Phylogeny showing the optimization of the third upper molar. Numbers on branches indicate node number. Green dots represent landmarks. Red lines represent the transformation from the last ancestor of the taxa/node.

Figure S8. Phylogeny showing the optimization of the first upper molar. Numbers on branches indicate node number. Green dots represent landmarks. Red lines represent the transformation from the last ancestor of the taxa/node.

Figure S9. Phylogeny showing the optimization of the third lower molar. Numbers on branches indicate node number. Green dots represent landmarks. Red lines represent the transformation from the last ancestor of the taxa/node.

Figure S10. Phylogeny showing the optimization of the first lower molar. Numbers on branches indicate node number. Green dots represent landmarks. Red lines represent the transformation from the last ancestor of the taxa/node.

Table S1. Sampled specimens for each molar, including collection data.

Data S1. TPS file with the unaligned specimens. The file contains the data of the four molars analysed here.